Journal of The Electrochemical Society

Performance and Durability of One-Cell Module of Biogas-Utilizing SOFC Equipped with Graded Indirect Internal Reformer

Journal of The Electrochemical Society, 2020 **167** 064512
1945-7111/2020/167(6)/064512/9/$40.00 © 2020 The Electrochemical Society ("ECS"). Published on behalf of ECS by IOP Publishing Limited

Performance and Durability of One-Cell Module of Biogas-Utilizing SOFC Equipped with Graded Indirect Internal Reformer

Özgür Aydın,[1,z] Go Matsumoto,[2] Atsushi Kubota,[2] Dang Long Tran,[3] Mio Sakamoto,[4] and Yusuke Shiratori[4,5]

[1]*Department of Mechanical Engineering, School of Engineering, Abdullah Gul University, Kocasinan, Kayseri, 38080, Turkey*
[2]*Department of Hydrogen Energy Systems, Graduate School of Engineering, Kyushu University, Nishi-ku, Fukuoka, 819-0395, Japan*
[3]*Department of Automotive Engineering, Ho Chi Minh City University of Technology, Ho Chi Minh City, Vietnam*
[4]*International Research Center for Hydrogen Energy, Kyushu University, Nishi-ku, Fukuoka, 819-0395, Japan*
[5]*Department of Mechanical Engineering, Faculty of Engineering, Kyushu University, Nishi-ku, Fukuoka, 819-0395, Japan*

Utilization of biogas in Solid Oxide Fuel Cells (SOFCs) is an efficient way of renewable power generation. Despite some technical challenges, biogas can be reformed to H_2-rich fuel stream in the anodes of SOFCs. However, the reforming rate drastically drops toward the outlet of the flow field due to the rapid conversion of CH_4 (biogas) in the inlet region. As the reforming reactions are endothermic, they cause large temperature gradients along the flow field, so that thermal stresses arise on the SOFC components. This problem can be resolved to an extent via taking the reforming reactions out of the SOFC domain (Indirect Internal Reforming), which however makes the heat transfer from SOFCs to the reforming domain also indirect. From the point of effective thermal integration, this study introduces an innovative indirect internal reforming concept. For totally eliminating the thermal stresses, it is necessary to homogenize the reforming rate, which can be achieved by designing a graded reforming domain. In this paper, we investigate the electrochemical performance and durability of an indirect internal reforming SOFC module featuring a graded reforming domain.
 [DOI: 10.1149/1945-7111/ab812c]

Manuscript submitted January 21, 2020; revised manuscript received March 10, 2020. Published April 2, 2020.

Although H_2 is to be utilized in fuel cells as the energy carrier for an environment-friendly power generation, the challenges associated with storing/distributing H_2 impede the adoption of fuel cells in the society. Therefore, on-site production (in fuel cell systems) of H_2 from hydrocarbons, such as CH_4, C_4H_{10}, etc., appears as an interim solution, as the infrastructure for distributing/storing hydrocarbon fuels is quite reliable.[1] Besides, ca. 96 % of H_2 is currently produced off-site (far from fuel cell systems) from hydrocarbons, albeit H_2 is projected to be extracted from H_2O by electrolysis powered by renewable sources.[2] Hence, on-site utilization of hydrocarbons in fuel cells is regarded as highly promising. Under current circumstances, bio-sources are highly valuable as renewable sources of hydrocarbons.[3–5] Among bio-sources, biogas (typically 60% CH_4 and 40% CO_2[6–8]) is broadly regarded as a reliable feedstock for on-site production of H_2 in fuel cell systems.

Thermodynamic considerations reveal that direct electrochemical oxidation of CH_4 (in biogas) yields a rather high energy conversion efficiency. The basis for the high conversion efficiency is the small entropy change, which however makes the electrochemical oxidation of CH_4 quite challenging. Hence, it is necessary to reform biogas to H_2 for utilizing in fuel cells.[9–13] In regard of biogas reforming, dry reforming (DR) appears more advantageous over steam reforming (SR) as well as other reforming (partial oxidation, autothermal) processes, as the reforming agent CO_2 inherently exists in biogas. In other words, an external supply of the reforming agent is required for other reforming processes, which is an additional balance of plant.

For reforming biogas, external reforming is a well-established technology and it can be employed for any fuel cell system. However, an external reforming process requires an external supply of thermal energy at an additional cost and complexity.[10,11] In fact, electrochemical energy conversion processes in fuel cells release thermal energy at significant rates.This waste heat can be used for reforming CH_4 in a system where the reforming domain can absorb the thermal energy from fuel cells; such a system increases the overall (electric and thermal) energy conversion efficiency significantly.

In terms of absorbing the thermal energy, there cannot be a better design than where the thermal energy is released and consumed. Indeed, in the anodes of SOFCs the CH_4 reforming reaction and the electrochemical oxidation of H_2 can occur simultaneously.This compact and efficient energy conversion system is known as Direct Internal Reforming SOFC (DIR-SOFC) and it offers great advantages: utilization of the excess heat and H_2O released by the electrochemical oxidation of H_2 for the endothermic reforming reactions, etc. With these great benefits, however, DIR-SOFCs become quite complicated. Thus, a reliable DIR-SOFC is yet to be accomplished due to serious challenges, e.g. carbon deposition, H_2S poisoning, inhomogeneous cooling, etc.[3,12–16]

Even though we cannot fully accomplish reliable DIR-SOFCs, we can approximate them to a great extent by an alternative concept referred to as Indirect Internal Reforming SOFCs (IIR-SOFC). As the name reveals, in an IIR-SOFC the reforming reactions are taken out of the SOFC domain into a separate reforming domain. However, the whole system is specifically designed for having the reforming domain to efficiently absorb the thermal energy released in the SOFC domain. This means that the thermal energy to be removed from the SOFC would be recuperated by the reforming reactions, and the energy needed for cooling the SOFC would be reduced. In this respect, we can say that IIR-SOFCs are as efficient as DIR-SOFCs. Furthermore, it is a fact that it is impossible to reform all CH_4 in the reforming domain due to thermodynamic (equilibrium) limitations. However, an IIR-SOFC allows for remaining CH_4 to pass into the subsequent SOFC domain, so that almost all CH_4 can be reformed.

In general, IIR-SOFCs reduce the complexity of DIR-SOFCs substantially, so that inhomogeneous cooling remains as the major challenge.[4,10,14,15,17–19] In a reforming domain featuring a uniform catalytic activity for a reasonable CH_4 conversion rate, the reforming process is usually completed in the inlet region.[4,10,14,15,17–19] In other words, the rest of the reforming domain remains passive. Since the reforming reactions are endothermic, temperature in the inlet region drops significantly comparing to the rest of the reforming domain, i.e. dramatic temperature gradients develop.[4,10,14,15,17–19] When the reforming domain is in intimate contact with the SOFC domain, the big temperature gradients induce large thermal stresses on the SOFC

[z]E-mail: ozgur.aydin@agu.edu.tr

components, which pose a high risk of mechanical failure of the SOFC domain.

Homogenizing the temperature distribution in the reforming domain appears as a sophisticated approach, which can be realized by grading the reforming domain. In this regard, tuning catalyst loading along the reforming domain is a quite practical method, for which division of the reforming domain into a number of segments (sub-domains) loaded with proper amounts of catalyst particles should be sufficient. Indeed, a long time ago Nagata et al. carried out a numerical study on a tubular SOFC equipped with a pre-reformer and an indirect internal reformer.[10] They graded the catalyst distribution in the indirect internal reformer and they found that the graded reforming domain reduced the temperature gradient over the SOFC. This study was later followed by a numerical study of an indirect tubular IIR-SOFC conducted by Nishino et al. where they also concluded that the temperature gradient over the cell can be reduced by adjusting the catalyst distribution.[20] Almost a decade later, Shiratori et al. carried out an experimental study of a graded catalyst distribution and presented feasibility of the method.[4] Recently Pajak et al. published a numerical study on a reactor where they adjusted the catalyst loading along the reactor and they pointed out that the temperature distribution was significantly improved with the graded design.[21] We also developed a reliable numerical model of a standalone reformer based on the in situ obtained experimental data for grading the reforming domain.[19] We were able to design a graded reforming domain with the developed model and verified the computed temperature profile with the experiments.

Relying on the model we developed for the standalone reformer, we attempted to demonstrate a durable power generation with a one-cell module of IIR-SOFC featuringa graded reforming domain. In this paper, we investigate the electrochemical performance and durability of the module. Besides, we analyze the temperature distribution in the reforming domain. According to the literature, this is the first paper demonstrating a durable power generation by an IIR-SOFC module equipped with a graded reforming domain and running on biogas.

One-Cell Module of IIR-SOFC

As sketched in Fig. 1, the one-cell module of IIR-SOFC contained a reforming domain and a SOFC domain. All the components of the module are displayed in Table I along with the respective materials and dimensions. The module was sitting on a Crofer® framework. While designing the module, we paid special attention to the effective transfer of the thermal energy from the SOFC domain to the reforming domain (the endothermic DR reaction).[16] Hence, the reformer was designed to sit directly on top the anode of the SOFC.

The dimensions of the reforming domain was 55/24/5 mm (length/width/height). It was surrounded by a holder and a top plate that accommodated small holes (0.7 mm) through which thermocouples were inserted. The thermocouples were fixed by a ceramic sealant (ARON Ceramic, Japan). The holder and the top plate of the reformer were both made of Crofer®. As the core elements of the reforming domain, PSC (Paper-Structured Catalysts) segments were placed directly on top of the anode current collector. Comprehensive information about PSCs is provided elsewhere.[19] In this design, the biogas entering the reformer arrives at the anode inlet as a H_2-rich gas mixture after reforming along the PSC segments (Fig. 1).

The SOFC domain contained an electrolyte; current collectors, support layers, and functional layers of the anode and cathode. The electrolyte of the cell was made of YSZ at a thickness of 3 μm. The current collectors of the anode and cathode were both made of Crofer® at 1 mm thickness. The anode support layer and the anode functional layer were made of Ni-YSZ at thicknesses of 300 μm and 20 μm, respectively. The cathode support layer and the cathode functional layer were made of LSC at thicknesses of 200 μm and 20 μm, respectively. The cathode support layer and the cathode functional layer were 50/20 mm (length/width), whereas the other components were 60/30 mm (length/width). Namely, the active area of the cell was 10 cm^2. While the SOFC (anode/electrolyte/cathode) was fabricated by Elcogen AS (Estonia), the other module components were manufactured by Magnex Co. Ltd. (Japan).

The module also included supplementary components of spacers (2 pieces) and insulators (3 pieces) which were made of Crofer® and MICA, respectively. The spacers were employed for homogenizing the in-plane pressure distribution on the components, whereas the insulators were used for inhibiting the electrical shortcuts as well as the gas leakage. A mesh made of Crofer® was also placed between the cathode and cathode current collector for damping the clamping pressure.

For minimizing the gas leakage and the electrical contact resistance between the electrodes and current collectors of anode and cathode, the module was clamped from the top plate of the reformer to the framework by multiple screws.

Measurements.—For controlling the temperature of the module during the experimental investigations a hotbox (Fig. 2) was employed. NiO catalyst particles of (Ni,Al,Mg)Ox solid solution (hydrotalcite dispersed in the PSCs), and the NiO particles in the anode of the module were reduced at ca. 1073 K by supplying pure H_2 at 100 ccm (25 K, 1 atm) for 15 h.

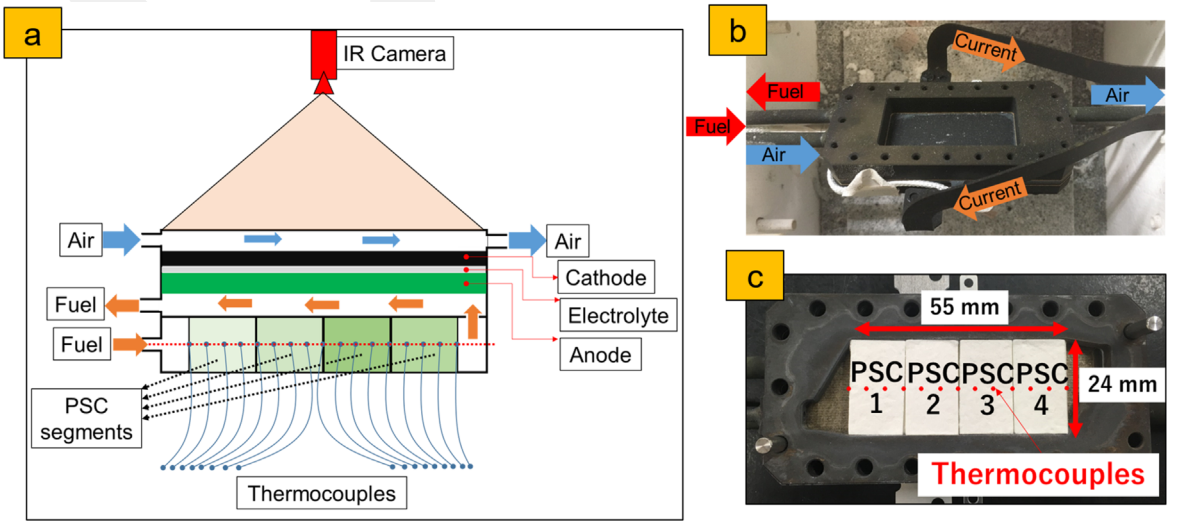

Figure 1. (a) Schematic (b) picture and (c) the reforming domain of the one-cell module of IIR-SOFC.

Table I. The components of the IIR-SOFC module listed along with the materials they were made of. The outer dimensions of all the components were 98/48 mm (length/width) except the electrochemical domain's components which are indicated in the table.

Component	Material	Thickness (mm)	Length/Width (mm)
Reformer top plate	Crofer®	1	
Reformer frame	Crofer®	5	
Insulator-1	Mica	0.5	
Anode current collector	Crofer®	1	
Spacer-1	Crofer®	0.3	
Anode	NiO/YSZ	0.3	60/30
Electrolyte	YSZ	0.003	60/30
Insulator-2	Mica-2	0.15	
Spacer-2	Crofer®	0.3	
Cathode mesh	Crofer®	0.7	50/20
Cathode	GDC/LSC	0.02	50/20
Cathode current collector	Crofer®	1	
Insulator-3	Mica	0.5	
Framework	Crofer®	9.6	

The experiments were conducted with the streams of simulated dry biogas ($CH_4/CO_2/N_2$) and H_2/N_2. However, the durability experiments were carried out with a stream of wet biogas ($CH_4/CO_2/N_2/H_2O$). 180 ccm was determined as the total flow rate (Gas Hourly Space Velocity) of the biogas. Single biogas composition was determined, where the flow rate of CH_4 was 40 ccm. Since the reforming rate maximizes with anequimolar supply of the biogas species, the molar ratio of CH_4/CO_2 was determined as the unity.[22,23] Considering the DR reaction in the reformer with a practical CH_4 conversion rate of 90%,[19] the flow rate for H_2/N_2 was calculated at the inlet of the anode and referred to as "equivalent" flow rate of the dry biogas. The reference investigations were conducted with the equivalent flow rate (IIR-SOFC experiments). With these considerations the investigations were carried out with the flow rates displayed in Table II.

The temperature distribution in the reformer was in situ measured by the thermocouples inserted along the PSC segments (Figs. 1 and 2). The thermocouples were positioned in the centerline (height and width) of the reforming domain with equal intervals (3.5 mm) along the flow field. The catalytic activity of the reforming domain (CH_4 conversion rate) was investigated via analyzing the composition of the exhaust gas by an automatic gas chromatograph (GC) (GC-20B, Shimadzu, Japan). Amount of the nickel catalysts in the PSC segments (wt%) was identified by ICP (Inductively Coupled Plasma) measurements.

The electrochemical characterization of the module was carried out by a potentiostat connected to the anode and cathode current collectors via "Four Point Probe" method. The measurements were conducted at the galvanostatic mode (constant current) and the electrochemical performance of the module is evaluated based on the current (density)/voltage plots. More insights into the electrochemical performance of the module was gathered via analyzing the ohmic (IR) loss and the overvoltage, which contains the voltage-losses asssociated with the activation of the electrochemical reaction and with the mass transport limitation.

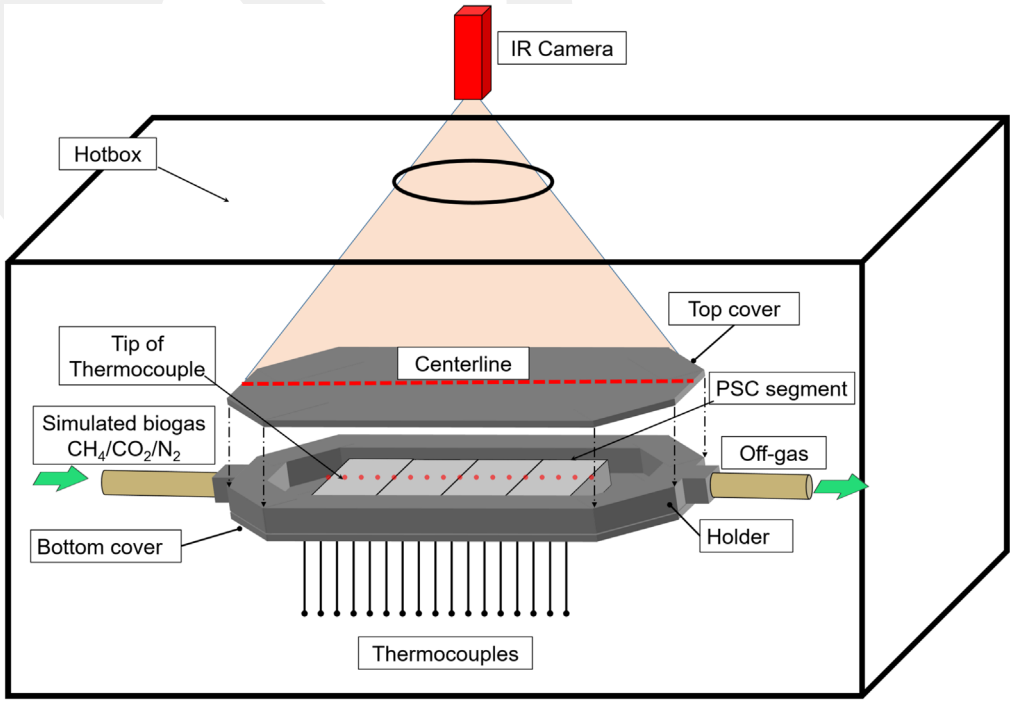

Figure 2. Schematic of the experimental setup with the standalone reformer.[19] In the case of the IIR-SOFC experiments, the standalone reformer was replaced by the IIR-SOFC module (Fig. 1).

Table II. The compositions of the inlet fuel streams and the rates at which the gas species were fed to the module.

Composition	Fuel mixture	Flow rate (ccm)
$CH_4/CO_2/N_2$	Dry biogas	40/40/100
$CH_4/CO_2/N_2/H_2O$	Wet biogas	40/40/82/18
H_2/N_2	Equivalent of dry biogas	72/108

Numerical model.—Even though our ultimate goal is to build a stack of IIR-SOFC containing multiple SOFCs and reformers, designing a graded reforming domain for a uniform temperature distribution in a stack is quite challenging. Thus, we preferred designing the graded reforming domain in a standalone reformer.[19] The physical properties of the standalone reformer and the reformer of the IIR-SOFC module were the same (Fig. 2). Namely, we carried out numerical and experimental studies on the reformer of the IIR-SOFC. Upon establishing a uniform temperature distribution in the reformer with a graded reforming domain, we integrated the reformer into the IIR-SOFC module and conducted experimental investigations.

Model validation.—For leveling the temperature distribution along the reforming domain, it was necessary to minimize the variation in the reforming rate, which could be achieved by grading the catalyst loading along the flow direction. Designing a graded reforming domain was the most challenging part of this study, for which we previously developed a strategy that can be summarized as follows.[19]

Initially we in situ measured the interior and surface temperature of the standalone reformer along the uniform reforming domain. Besides, we modelled the experimental setup in COMSOL Multiphysics and validated this FEM model with the interior and surface temperature profiles of the reformer via adjusting the relevant parameters. For ensuring reliability of the model, we measured the temperature profiles of the uniform reforming domain for two other nickel loading conditions and investigated accuracy of the computations for these conditions. For these investigations, we altered solely the pre-exponential factor of the rate coefficient as it represents the catalyst loading. Good agreements among the numerical and experimental temperature profiles allowed us to confirm reliability of the model and it allowed us to derive a relationship between the pre-exponential factor and the catalyst loading. Deriving this relationship was the most crucial part of the study, as it became the basis for designing graded reforming domains. Eventually we numerically designed a highly homogenized temperature profile in the reformer via grading the reforming domain and experimentally verified the homogenized temperature profile.

Results and Discussion

Temperature distribution in the SOFC components with indirect internal reforming.—For ensuring the durable power generation in biogas-utilizing SOFCs, we introduced two measures by the indirect internal reformer featuring a graded reforming domain. The first measure refers to moving the reforming reactions away from the anode of the SOFC, i.e. changing the operation from DIR to IIR. With this measure, a thermal impedance was introduced between the reforming domain and the SOFC domain. According to Fig. 3, the thermal impedance reduced the impact of the drastically changing reforming rate on the temperature distribution of the SOFC components to a great extent.

In Fig. 3 we can see the computed temperature profile along the uniform reforming domain at various thicknesses from the bottom of the reformer. In the uniform domain nickel loading was 0.22 wt% as the minimum amount for a sufficient CH_4 conversion rate[23]. Note that the computations were executed with the validated model described by Aydın et al.[19] According to the computations, the greatest temperature gradient appears at 3-4 mm thickness in the inlet region (ca. 3 mm) due to the highest reforming rate. If this was a DIR process, a similar temperature drop would develop within the anode of the SOFC domain, which would result in large thermal stresses on the adjacent components. The temperature profiles at the other thicknesses display that the temperature gradient reduces toward the top and bottom boundaries of the reformer (Fig. 2). The difference between the max. and min. temperatures on the bottom surface of the reforming domain is approximately 8 degree. The variation of the temperature profile across the thickness of the reforming domain is related to various parameters, such as the low thermal conductivity and high porosity of PSC segments, the high thermal conductivity of top and bottom plates of the reformer, and the high radiation heat transfer on the top and bottom surfaces.[19] Leaning upon these evidences, we anticipate even smaller temperature gradients over the SOFC components of the IIR-SOFC, as there is also a fuel stream between the reforming domain and the SOFC components, which is an additional impedance to the heat transfer.

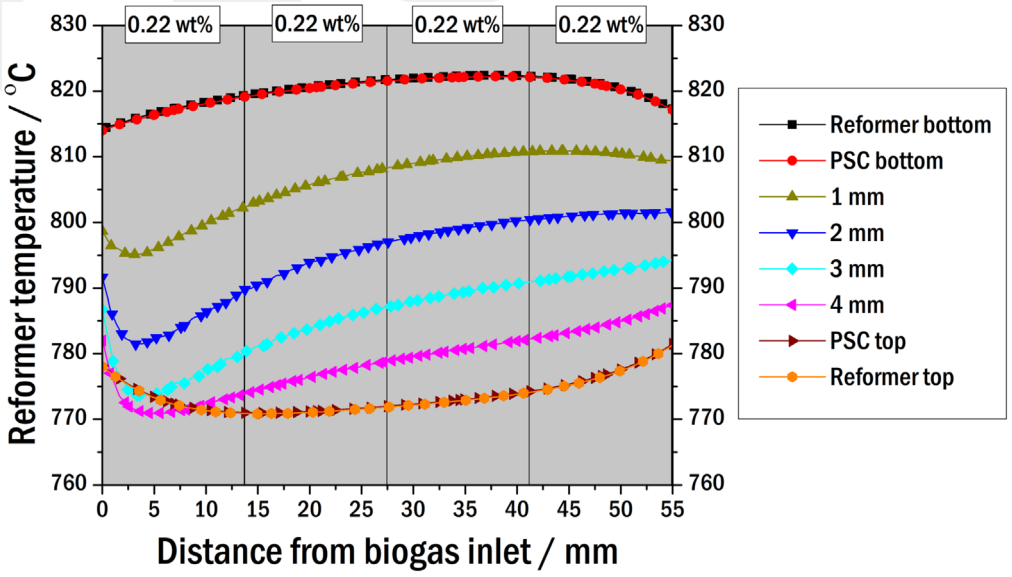

Figure 3. For 40 ccm ($CH_4/CO_2/N_2 = 40/40/100$ ccm) the temperature distribution along the uniform reforming domain (0.22 wt% nickel loading) at various distances from the bottom of the reformer (Fig. 2). Note that the computations were executed with the validated model described by Aydın et al.[19]

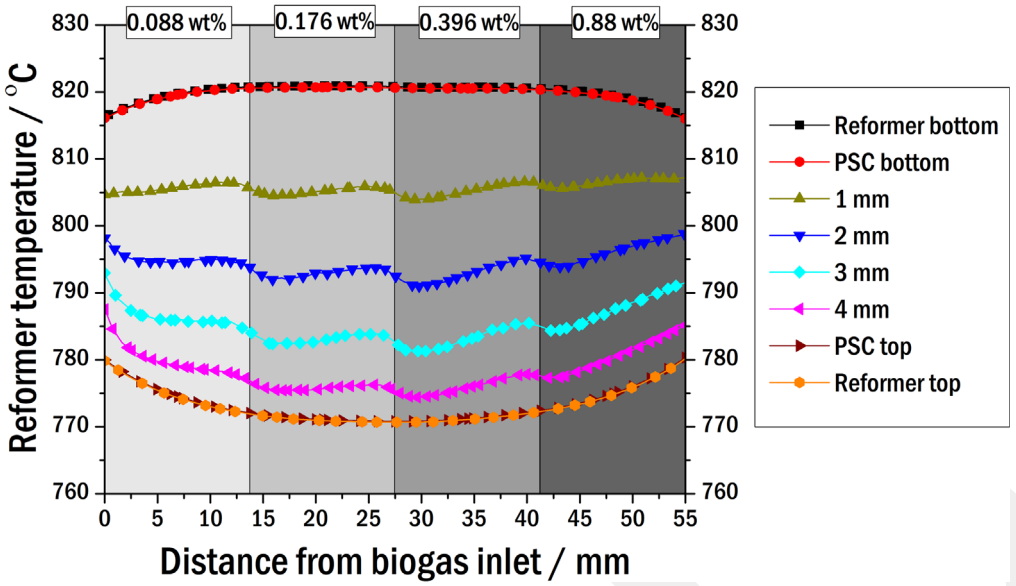

Figure 4. For 40 ccm ($CH_4/CO_2/N_2 = 40/40/100$ ccm) the temperature distribution along the graded reforming domain (0.088, 0.176, 0.396, 0.88 wt% nickel loading) at various distances from the bottom of the reformer(Fig. 2). Note that the computations were executed with the validated model described by Aydın et al.[19]

The second measure refers to designing a graded reforming domain for minimizing the variation in the reforming rate. By grading the reforming domain, the quick variation in the reforming rate (Fig. 3) can be reduced, so that the temperature gradient can be minimized.[19] This prevents development of the thermal stresses on the SOFC components, so that a durable power generation can be achieved.

Figure 4 shows the computed temperature profiles along the graded reforming domain at varying thicknesses from the bottom of the reformer (Fig. 2). It is evident that by grading the reforming domain temperature gradients in the reformer were significantly reduced. Hence, the temperature profile along the reformer became flatter at every thickness. This evidence indicates that the reforming rate in the inlet of the reformer was restricted to a great extent, so that the reforming reaction proceeded at a sustainable rate along the reforming domain. As a result, the temperature gradients almost disappear around the top/bottom boundaries of the reformer. The difference between the max. and min. temperatures on the bottom surface of the reforming domain reduces (comparing to the uniform domain) to 4 degree. Recalling the thermal impedance present between the reformer and the SOFC domain due to the fuel stream, we do not anticipate any thermal stress on the SOFC components with the graded reforming domain.

Preceding analyses indicated that taking the reforming reactions out of the anode of the SOFC domain, i.e. changing the operation from DIR to IIR, and grading the reforming domain minimizes the risk of the mechanical failure of the SOFC components. These findings encouraged us for experimentally investigating the performance of the IIR-SOFC module by integrating the reformer into the SOFC domain.

In Fig. 5, we can analyze the computed and measured temperature profiles of the graded reforming domain when the module was fed by the dry biogas. Note that the temperature data are not available after 50 mm due to the failure of the TCs during experiments. However, the lack of the temperature data in that range does not affect the analysis very much, as the crucial part of the reforming domain is the inlet vicinity. It is visible that the numerical and experimental temperature profiles are resembling with insignificant deviations. This finding verifies the current modeling approach and it indicates that it is possible to design graded reforming domains separately on a standalone reformer for building IIR-SOFC modules/stacks.

For revealing advantages of the graded reforming domain, Fig. 5 presents also the temperature profile measured along the uniform (0.22 wt%) reforming domain when the module was fed by the dry biogas. We can see that the max. temperature gradient is much bigger with the uniform reforming domain. This means that in a long term operation consequences of the thermal stresses arising due to temperature gradients will be greater with the uniform reforming domain.

As stated previously, designing a graded reforming domain for a uniform temperature distribution in a stack is quite challenging. Thus, we preferred designing a graded reforming domain in a standalone reformer (Fig. 2) which did not consider two main contributions that affect the energy balance of the IIR-SOFC module: one of them is the thermal energy released by the SOFC domain and the other one is the convective heat transfer taking place between the cathode surface and the air flow. Since the released

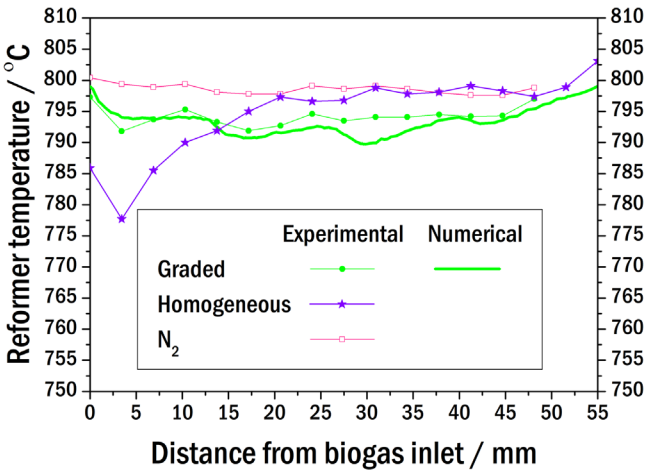

Figure 5. In the reformer mode (no current and no air flow) the temperature distribution along the reforming domain of the IIR-SOFC module compared in terms of the design of the reforming domain for $CH_4/CO_2/N_2 = 40/40/100$ ccm. The uniform reforming domain was fabricated by 0.22 wt% nickel loading, whereas the graded reforming domain was designed with 0.088, 0.176, 0.396, 0.88 wt% nickel loading. During the purging process N_2 flow rate was 100 ccm.

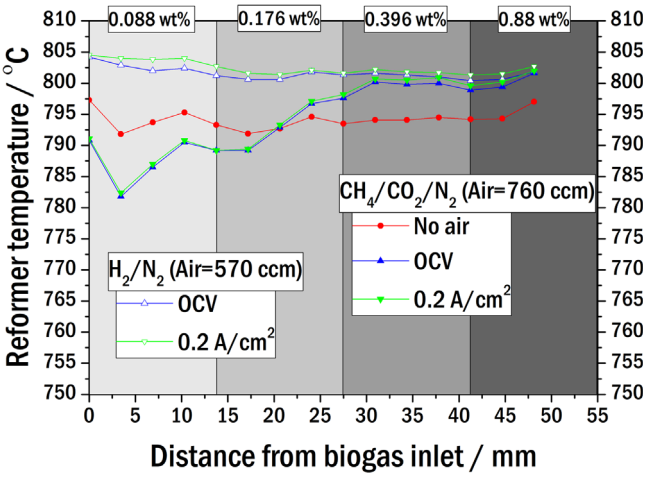

Figure 6. Impact of the current density on the temperature distribution along the reforming domain of the IIR-SOFC module plotted for $CH_4/CO_2/N_2 = 40/40/100$ ccm and equivalent $H_2/N_2 = 72/108$ ccm when the reforming domain was graded (0.088, 0.176, 0.396, 0.88 wt%). During the purging process N_2 flow rate was 100 ccm.

thermal energy is proportional to the current density of the SOFC domain, we investigated the impact of the electrical load on the temperature profile of the reformer and plotted in Fig. 6. In this figure, we see that the temperature profile at 0.2 A cm^{-2} with the dry biogas stream almost overlaps the temperature profile recorded with the identical fuel stream under the open-circuit voltage (OCV) condition. The impact of the electrical load is almost the same in the case of H_2/N_2 stream; the temperature profiles under 0.2 A cm^{-2} and the OCV conditions are almost overlapping. Thus, we can say that the impact of the electrical load on the temperature profile of the reforming domain is negligible in this current density range (it may be large at higher current density). Nonetheless, we anticipate greater temperature gradients on the SOFC components, which do not appear in the reforming domain due to the presence of the thermal impedance (the fuel stream) between the reforming and the SOFC domains.

Figure 6 presents also the temperature profile of the IIR-SOFC measured in the reformer mode (no air flow). This allows us to analyze the impact of the air flow on the temperature profile of the reformer. When the module was fed by air (OCV and 0.2 A cm^{-2}), temperature reduced in the inlet part of the reforming domain (0–20 mm), whereas it increased considerably toward the outlet (20–55 mm). Knowing that biogas and air both flow in the same direction (Fig. 1), the considerable change in the temperature profile can be attributed to the effective convective heat transfer occurring at the cathode side.[24] Since the air flow rate (flow velocity) was smaller with the stream of H_2/N_2, the impact of the air flow was negligible.

Electrochemical performance of the module with indirect internal reforming.—Table III indicates the fuel compositions at the inlet and outlet of the IIR-SOFC module in the reformer mode (no current and no air). It is visible that both uniform and graded reforming domains yield approximately the same fuel compositions at the inlet of the anode in the absence of H_2O, albeit the uniform domain yields more H_2. We understand from this table that the fuel streams were fed to the module at equivalent rates, i.e. our estimations for the equivalent rates of fuel streams were accurate. On this basis, we expect an identical electrochemical performance from the module regardless of the reforming domain. This expectation can be discussed on Figs. 7 and 8.

In Fig. 7a the current-voltage (iV) curve of the module equipped with a uniform reforming domain is compared for the dry and wet biogas streams as well as for the equivalent H_2/N_2. All the fuel streams were supplied to the module at the equivalent flow rates (Table II). We see that the fuel stream of H_2/N_2 indicates the greatest OCV. The dry biogas yields a smaller OCV due to the existence of other species (CO, CO_2, etc.). The wet biogas manifests the smallest OCV due to the presence of H_2O, despite the higher concentration of H_2.

H_2O was added to the dry biogas for preventing carbon deposition on the nickel particles in the reforming domain. It was stated previously that the equimolar composition of the dry biogas was determined for maximizing the CH_4 conversion rate leaning upon the preceeding studies [22,23] In those studies, they pointed out that no carbon deposition occurred under the equimolar supply of biogas species. Since their investigations were on DIR-SOFCs, the reason for the carbon deposition in the reforming domain of the current study is attributed to the lack of H_2O, i.e. in the case of DIR-SOFC, the electrochemically produced H_2O assists the reforming process.[22,23]

When the iV curves of the module were analyzed, we understand that the module performs very similar with the dry and wet biogas streams despite the greater OCV measured with the dry biogas . These similar performances are attributed to the fact that the partial conversion of CH_4 to H_2 for both of the fuel stream is completed in the anode with the electrochemically produced H_2O when the current density was greater than zero. Nonetheless, the performance of the module is the best with H_2/N_2 due likely to the smallest IR loss owing to the highest operating temperature (Fig. 6).

Figure 7b provides more insights into the variation in the electrochemical performance of the module with respect to the fuel stream. In the figure the IR loss and the overvoltage measured with the uniform reforming domain are plotted for all the fuel streams. It is interesting to observe variations in the IR loss with respect to the fuel stream. It seems that the module indicates similar IR losses with the dry and wet biogas streams, whereas it exhibits a smaller IR loss with the fuel stream of H_2/N_2. The greater IR losses with the dry and wet biogas streams can be attributed to the smaller average operating temperature due to the temperature gradients (Fig. 5). We can also ascribe the overlapping IR losses to the very similar temperature profiles over the components of the module with dry and wet biogas due to the fact the reforming process was limited by the catalyst loading. More explicitly, the addition of H_2O slightly changed the gas composition at the reformer outlet (less CO_2 was consumed, Table III). Hence, the consumed thermal energy was little affected by the different enthalpy changes of the dry ($\Delta H_{298K} = 247$ kJ mol^{-1}) and steam ($\Delta H_{298K} = 206$ kJ mol^{-1}) reforming reactions. We believe that the IR losses measured with the dry and wet biogas streams could be reduced if we set the operating temperature higher at which the mean temperature would be close to that is observed with H_2/N_2. From these findings we understand that the temperature profile in the reforming domain affects the temperature field in the SOFC domain. However, the effect can be tolerated in terms of electrochemical performance.

In Fig. 7b the overvoltages are also distinguished from each other with respect to the fuel stream. We can see that the overvoltage with the fuel stream of H_2/N_2 is the greatest comparing to the overvoltages of the other fuel streams. As the overvoltage arises due to the activation resistance and mass transport limitation, the smaller overvoltages with the dry and wet biogas streams can be attributed to the boosted concentration of H_2 in the anode by the further conversion of CH_4 and CO via steam reforming and water-gas-shift reactions. Since the concentration of H_2 in the reformer mode (Table III) is equal ($CH_4/CO_2/N_2$) or greater ($CH_4/CO_2/N_2/H_2O$) than that is supplied by H_2/N_2, it will definitely enhance within the anode compartment by the aforementioned reactions. Because the dry and wet biogas streams contain the same amount of CH_4, the smallest overvoltage measured with the stream of wet biogas is attributed to the positive impact of H_2O on the activation overvoltage.[25]

We repeated the previous analyses when the reforming domain was graded. Figure 8a illustrates the electrochemical performance of

Table III. In the reformer mode (no current) CH_4 conversion rates measured by GC for different inlet compositions.

	Inlet Gas				Outlet Gas Composition						
Uniform	**Composition (ccm)**				**(ccm)**						
	CH_4	**CO_2**	**N_2**	**H_2O**	**H_2**	**O_2**	**N_2**	**CH_4**	**CO**	**CO_2**	**CH_4 Conversion Rate (%)**
	40	40	100	0	71	1	100	5	74	4	88
	40	40	82	18	86	1	82	2	76	12	96
	Inlet Gas				**Outlet Gas Composition**						
Graded	**Composition (ccm)**				**(ccm)**						
	CH_4	**CO_2**	**N_2**	**H_2O**	**H_2**	**O_2**	**N_2**	**CH_4**	**CO**	**CO_2**	**CH_4 Conversion Rate (%)**
	40	40	100	0	67	1	100	5	72	3	89
	40	40	82	18	77	1	82	3	74	16	93

the module for H_2/N_2, $CH_4/CO_2/N_2$, and $CH_4/CO_2/N_2/H_2O$, which were fed to the module at the equivalent flow rates. We see that the fuel stream of H_2/N_2 manifests the highest OCV while the wet biogas stream yields the smallest OCV due to the existence of H_2O (Nernst equation), despite the higher concentration of H_2 (Table III). We note that the dry biogas stream exhibits an OCV that is comparable to the OCV recorded with H_2/N_2. This suggests that the existence of the other species (CO, CO_2, etc.) have negligible impact on the OCV of the IIR-SOFC module.

When we look at the iV curves, we understand that the module performs very similar regardless of the fuel stream. Nonetheless, the module experiences a rapid voltage-drop with H_2/N_2 after 0.3 A cm^{-2}. The better performance of the module with the dry and wet biogas streams can be attributed to the further conversion of CH_4 and CO in the anode by the steam reforming and water-gas-shift reactions.

Figure 8b displays the overvoltages and the IR losses of the module with respect to the fuel stream. Even though the IR losses recorded with the dry and wet biogas streams overlap, they are greater than the IR loss recorded with the stream of H_2/N_2. This difference can be ascribed to the lower mean operation temperature experienced with the streams of dry and wet biogas (Fig. 5).

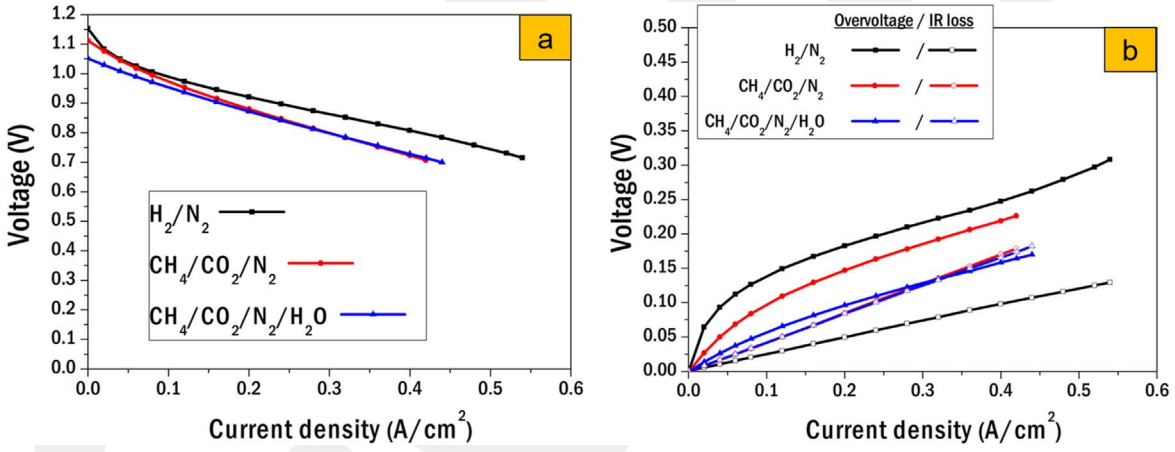

Figure 7. (a) iV curves and (b) voltage-losses of the IIR-SOFC module measured for $H_2/N_2 = 72/108$ ccm, $CH_4/CO_2/N_2 = 40/40/100$ ccm, and $CH_4/CO_2/N_2/H_2O = 40/40/82/18$ ccm when the reforming domain contained homogeneous nickel particles (0.22 wt%). All the experiments were carried out with an air flow rate of 500 ccm.

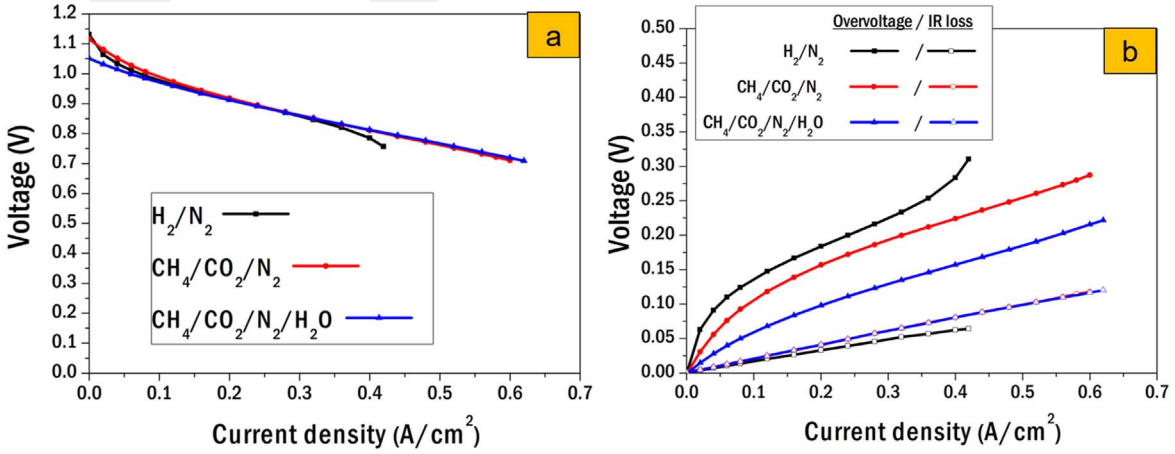

Figure 8. (a) iV curves and (b) the voltage-losses of the IIR-SOFC module measured for $H_2/N_2 = 72/108$ ccm, $CH_4/CO_2/N_2 = 40/40/100$ ccm, and $CH_4/CO_2/N_2/H_2O = 40/40/82/18$ ccm when the reforming domain was designed with 0.088, 0.176, 0.396, 0.88 wt% nickel loading. All the experiments were carried out with an air flow rate of 500 ccm.

When it comes to the overvoltage of the module measured with regard to the fuel stream, we think that the mass transport limitation dominates. The module exhibits lower overvoltages with the dry and wet biogas streams. However, the overvoltage is the smallest with the wet biogas. This is due to firstly the augmented CH_4 conversion rate by the steam reforming and the water-gas-shift reactions occurring in the anode and secondly due to the positive impact of H_2O on the activation overvoltage.[25] From these findings we understand that the dry and wet biogas streams yield greater H_2 concentrations in the anode than what we initially estimated.

Comparison of Figs. 7a and 8a reveals that the module exhibits a better performance with the dry and wet biogas streams when the reforming domain was graded. However, we cannot ascribe the better performance of the module to the reduced temperature gradients of the reformer by grading the reforming domain, because the IR loss with the stream of H_2/N_2 is also smaller for the graded reforming domain. In other words, if the total contact resistance among the components of the IIR-SOFC modules equipped with the uniform and graded reforming domains was the same, both modules would manifest identical IR losses with the stream of H_2/N_2. The greater IR loss with the IIR-SOFC module accommodating the uniform reforming domain is hence attributed to the assembly process.

Durability of the module with indirect internal reforming.— According to Figs. 7 and 8 the temperature distribution in the reforming domain does not make a big impact on the electrochemical performance of the module. However, the thermal stresses arising due to the temperature gradients on the SOFC components reportedly prompt crack formation in the components that leads to termination of the electrochemical energy conversion process.[4] Indeed, this study was dedicated to mitigation of the temperature gradient on the SOFC components. The numerical data displayed in Figs. 3 and 4 indicated that shifting the operation from DIR to IIR reduced the impact of the drastically changing reforming rate on the temperature distribution of the SOFC components. Nonetheless, we suspected on the long-term durability of the IIR-SOFC module equipped with a uniform reforming domain due to the greater temperature gradients.

Figure 9 illustrates the durability of the module along with the voltage-losses with respect to the design of the reforming domain for 200 hrs. Generally the module exhibits quite similar performance with both designs of the reforming domain, except that the rate of the degradation is higher (almost double) with the uniform reforming domain. The voltage difference between the uniform and graded reforming domains for the identical current density can be attributed to the different IR losses and overvoltages (including the activation and mass transfer resistances), as plotted in Fig. 10.

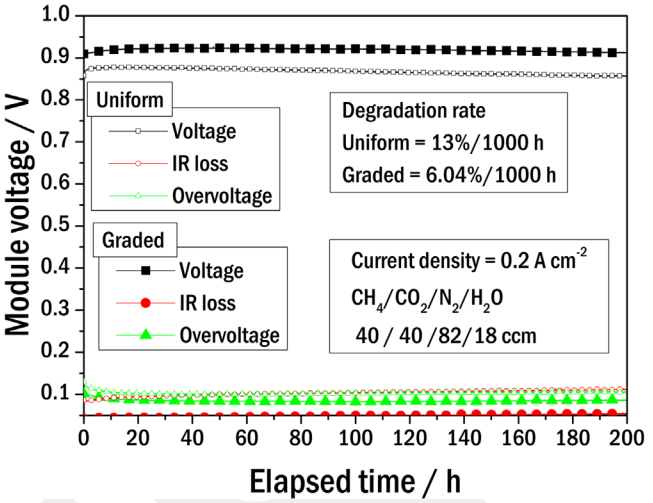

Figure 9. The cell voltage, IR loss and overvoltage of the SOFC domain of the IIR-SOFC module recorded and compared at 0.2 A cm^{-2} for the uniform (0.22 wt% nickel loading) and graded reforming domains (0.088, 0.176, 0.396, 0.88 wt% nickel loading). The tests were carried with the fuel stream of $CH_4/CO_2/N_2/H2_O = 40/40/82/18$ ccm and with an air stream of 500 ccm.

According to Fig. 9, in the first 10 hrs an evident rise in the cell voltage appears regardless of the reforming domain. The voltage rises are apparently consequences of the drops in the overvoltages (Fig. 10b), which can be ascribed to the lagging activation of the cathode.[26]

In the next stage of the time-frame, we see a slightly increasing IR loss with the graded reforming domain. However, the uniform reforming domain causes growth in the IR loss as well as in the overvoltage of the module. Therefore, the module exhibits a noticeable performance degradation with the uniform reforming domain. Having the same SOFC components and similar fuel compositions at the anode inlet, only the temperature distribution appears as the main difference between the uniform and the graded reforming domains. As Fig. 5 depicts, the uniform domain exhibits much bigger temperature gradients which are suspected to prompt micro-crack formation. As a result, the IR loss and the overvoltage of the module increase with time while the cell voltage declines. Thus, we can conclude that a durable power generation by the IIR-SOFC is not possible with the uniform reforming domain.

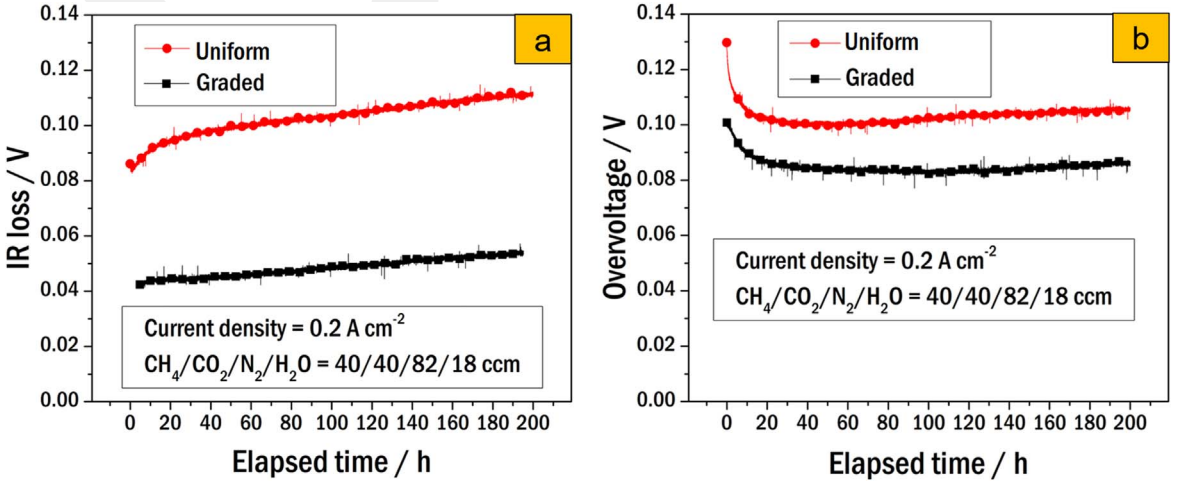

Figure 10. (a) IR loss and (b) overvoltage of the SOFC domain of the IIR-SOFC module compared at 0.2 A cm^{-2} for the uniform (0.22 wt% nickel loading) and graded (0.088, 0.176, 0.396, 0.88 wt% nickel loading) reforming domains. The tests were carried with an air stream of 500 ccm.

Conclusions

This study was dedicated to demonstrate a durable operation of a one-cell Solid Oxide Fuel Cell (SOFC) module utilizing biogas reformed through a graded reforming domain of an indirect internal reformer. By comparing the electrochemical performances and the temperature distributions over the components of the module equipped with a graded reforming domain to that of the module equipped with a uniform reforming domain, advantages of the graded reforming domain are revealed. The comparative investigations led to the following conclusions:

- In comparison to direct internal reforming, indirect internal reforming significantly reduces thermal stresses developing on the SOFC components,
- A durable power generation by indirect internal reforming SOFCs requires oxidant addition for avoiding the carbon deposition occurring at the equimolar supply of CH_4 and CO_2,
- Despite the alleviated temperature gradient on the SOFC components by indirect internal reforming, the uniform reforming domain causes degradation,
- Graded reforming domains may be useful for a sustainable power generation by indirect internal reforming SOFCs ,
- For building indirect internal reforming SOFC stacks with graded reforming domains, design of the reforming domain on a representative (standalone) reformer is sufficient.

Acknowledgments

This work was supported by JSPS KAKENHI Grant Number JP17H03185. A part of Dr. Aydın's contribution to this research was supported by "Postdoctoral Fellowship of JSPS (Japanese Society for the Promotion of Science)".

ORCID

Özgür Aydın https://orcid.org/0000-0002-8814-6025

References

1. A. L. Dicks, "Hydrogen generation from natural gas for the fuel cell systems of tomorrow." *J. Power Sources*, **61**, 113 (1996).
2. M. Keane, M. K. Mahapatra, A. Verma, and P. Singh, "LSM-YSZ interactions and anode delamination in solid oxide electrolylsis cells." *Int. J. Hydrogen Energy*, **37**, 16776 (2012).
3. Y. Shiratori, T. Ijichi, T. Oshima, and K. Sasaki, "Internal reforming SOFC running on biogas." *Int. J. Hydrogen Energy*, **35**, 7905 (2010).
4. Y. Shiratori, T. Ogura, H. Nakajima, M. Sakamoto, Y. Takahashi, Y. Wakita, T. Kitaoka, and K. Sasaki, "Study on paper-structured catalyst for direct internal reforming SOFC fueled by the mixture of CH4 and CO2." *Int. J. Hydrogen Energy*, **38**, 10542 (2013).
5. Y. Shiratori, T. Quang-Tuyen, and K. Sasaki, "Performance enhancement of biodiesel fueled SOFC using paper-structured catalyst." *Int. J. Hydrogen Energy*, **38**, 9856 (2013).
6. Y. Shiratori, T. Oshima, and K. Sasaki, "Feasibility of direct-biogas SOFC." *Int. J. Hydrogen Energy*, **33**, 6316 (2008).
7. H. J. Alves, C. B. Junior, R. R. Niklevicz, E. P. Frigo, M. S. Frigo, and C. H. Coimbra-Araújo, "Overview of hydrogen production technologies from biogas and the applications in fuel cells." *Int. J. Hydrogen Energy*, **38**, 5215 (2013).
8. J. Huang and R. J. Crookes, "Assessment of simulated biogas as a fuel for the spark ignition engine." *Fuel*, **77**, 1793 (1998).
9. E. Achenbach and E. Riensche, "Methane/steam reforming kinetics for solid oxide fuel cells." *J. Power Sources*, **52**, 283 (1994).
10. N. Susumu, A. Momma, T. Kato, and Y. Kasuga, "Numerical analysis of output characteristics of tubular SOFC with internal reformer." *J. Power Sources*, **101**, 60 (2001).
11. G. Brus and J. S. Szmyd, "Numerical modelling of radiative heat transfer in an internal indirect reforming-type SOFC." *J. Power Sources*, **181**, 8 (2008).
12. Y. Shiratori, M. Sakamoto, T. Uchida, H. Le, T. Quang-Tuyen, and K. Sasaki, "Hydrotalcite-dispersed paper-structured catalyst for the dry reforming of methane." *Int. J. Hydrogen Energy*, **40**, 10807 (2015).
13. Y. Shiratori and M. Sakamoto, "Performance improvement of direct internal reforming solid oxide fuel cell fuelled by H2S-contaminated biogas with paper-structured catalyst technology." *J. Power Sources*, **332**, 170 (2016).
14. Ö. Aydın, H. Nakajima, and T. Kitahara, "Current and temperature distributions in situ acquired by electrode-segmentation along a microtubular solid oxide fuel cell operating with syngas." *J. Power Sources*, **293**, 1053 (2015).
15. J. D. Kirtley, D. A. Steinhurst, J. C. Owrutsky, M. B. Pomfret, and R. A. Walker, "In situ optical studies of methane and simulated biogas oxidation on high temperature solid oxide fuel cell anodes." *Phys. Chem. Chem. Phys.*, **16**, 227 (2014).
16. A. Lanzini and P. Leone, "Experimental investigation of direct internal reforming of biogas in solid oxide fuel cells." *Int. J. Hydrogen Energy*, **35**, 2463 (2010).
17. D. Long Tran, Q. Tuyen Tran, M. Sakamoto, K. Sasaki, and Y. Shiratori, "Modelling of CH4 multiple-reforming within the Ni-YSZ anode of a solid oxide fuel cell." *J. Power Sources*, **359**, 507 (2017).
18. J. E. A. Saunders and M. H. Davy, "In-situ studies of gas phase composition and anode surface temperature through a model DIR-SOFC steam-methane reformer at 973.15 K." *Int. J. Hydrogen Energy*, **38**, 13762 (2013).
19. Ö. Aydın, A. Kubota, D. Long Tran, M. Sakamoto, and Y. Shiratori, "Designing graded catalytic domain to homogenize temperature distribution while dry reforming of CH4." *Int. J. Hydrogen Energy*, **43**, 17431 (2018).
20. T. Nishino, H. Iwai, and K. Suzuki, "Comprehensive numerical modeling and analysis of a cell-based indirect-internal reforming tubular SOFC." *J. Fuel Cell Sci. and Technol.*, **3**, 33 (2006).
21. M. Pajak, M. Mozdzierz, B. Chalusiak, S. Kimijima, J. S. Szmyd, and G. Brus, "A numerical analysis of heat and mass transfer processes in a macro-patterned methane/steam reforming reactor." *Int. J. Hydrogen Energy*, **43**, 20474 (2018).
22. I. V. Yentekakis, "Open- and closed-circuit study of an intermediate temperature SOFC directly fueled with simulated biogas mixtures." *J. Power Sources*, **160**, 422 (2006).
23. G. Goula, V. Kiousis, L. Nalbandian, and I. V. Yentekakis, "Catalytic and electrocatalytic behavior of Ni-based cermet anodes under internal dry reforming of CH4+CO2 mixtures in SOFCs." *Solid State Ionics*, **177**, 2119 (2006).
24. Ö. Aydın, H. Nakajima, and T. Kitahara, "Processes involving in the temperature variations in solid oxide fuel cells in situ analyzed through electrode-segmentation method." *J. Electrochem. Soc.*, **163**, F216 (2016).
25. S. H. Jensen, A. Hauch, P. V. Hendriksen, M. Mogensen, N. Bonanos, and T. Jacobsen, "A method to separate process contributions in impedance spectra by variation of test conditions." *J. Electrochem. Soc.*, **154**, B1325 (2007).
26. S. P. J. Jiang, "Activation, microstructure, and polarization of solid oxide fuel cell cathodes." *J. Solid State Electrochem*, **11**, 93 (2007).